DETECTION OF GEOMETRICALLY KNOWN TARGETS IN THROUGH-THE-WALL RADAR IMAGING

Christian Debes[1]*, Abdelhak M. Zoubir* [1] *and Moeness G. Amin*[2]

[1]Signal Processing Group
Technische Universität Darmstadt
Darmstadt, Germany

[2]Center for Advanced Communications
Villanova University
Villanova, PA, USA

ABSTRACT

We consider the problem of detecting targets behind walls using radar imaging technology. An image-domain based detection technique is proposed that allows to adapt to specific targets of interest. By doing so, clutter as well as targets of no-interest are strongly reduced in the radar image. The proposed detector is automatic in the sense that no or only little prior knowledge on the image statistics is required. The detection procedure is detailed, including the choice of suitable optimality criteria. The evaluation of the proposed technique is performed using data collected from Through-the-Wall radar imaging experiments whereby we specifically consider on the detection of humans.

Index Terms— Detection, Through-the-wall, Radar imaging

1. INTRODUCTION

In Through-the-Wall Radar Imaging (TWRI) [1, 2], radar technology is used to image scenes that are hidden behind visually opaque materials such as walls. TWRI is a key technology in numerous civilian, law enforcement and military applications where one is interested to obtain images from scenes that are non-accessible physically, optically, acoustically or thermally. In all those applications, the detection of humans is of primary interest, e.g., when it comes to resolving hostage crises, detecting buried humans after natural disasters or in obvious military scenarios.

Doppler signatures or change detection techniques [3, 4, 5, 6] can be applied when considering animate targets. The problem, however, becomes more challenging when the targets of interest are stationary. This may be the case for trapped humans in tightly enclosed structures, hostage situations or other inanimate targets such as furniture, concealed weapons, and explosives, etc. In this case, target detection is to be performed subsequent to image formation [1]. Images obtained from behind a wall using an antenna array and performing beamforming, however, are prone to strong distortions that complicate any post-processing method such as target detection, identification and classification. These distortions include, but not restricted to, uncompensated wall effects and multipath propagation.

The contribution of this paper is the development of a novel adaptive image domain-based detector that takes into account the respective target signatures. The new detector is based on our previous work [7, 8], where we derived a detection scheme that allows to automatically adapt to changing and unknown image statistics and which has been proven useful for target detection in TWRI. We follow a template-based scheme where, for a given target of interest, an optimal template is found that can be directly incorporated in the detection scheme.

The paper is structured as follows. In Section 2, we briefly review the iterative target detector from [7, 8], including a discussion on optimal settings. This detector is extended in Section 3 by introducing the concept of optimal templates for specific targets of interest. Experimental results are presented in Section 4, while Section 5 provides conclusions.

2. TARGET DETECTION IN THROUGH-THE-WALL RADAR IMAGING

In agreement with the experimental validation in Section 4, we restrict ourselves to two-dimensional TWRI images. All follow-on concepts can, however, be straightforwardly extended to three-dimensional TWRI images [7].

Let $Y(i,j)$ with $i = 0,...,N_i - 1$, $j = 0,...,N_j - 1$ denote the acquired TWRI image with i and j denoting the dimensions in crossrange and range, respectively. It is the aim of the image domain-based target detection to obtain a detector $B(i,j)$, $i = 0,...,N_i - 1$, $j = 0,...,N_j - 1$ with

$$B(i,j) = \begin{cases} 1, & \text{target present at}(i,j) \\ 0, & \text{target absent at}(i,j) \end{cases} \quad (1)$$

Let the images $Y(i,j)$ and $B(i,j)$, $i = 0,...,N_i - 1$, $j = 0,...,N_j - 1$ be represented for simplicity by the $(N_i \times N_j)$-matrices $\mathbf{Y}$ and $\mathbf{B}$. In a hypothesis testing framework, we

The work by Moeness Amin is supported by ONR, grant no N00014-07-C-0413

define the null and alternative and hypothesis pair H_0 and H_1 describing the absence and presence of a target. Further, let $p(\mathbf{Y}|H_0;\underline{\theta}_0)$ and $p(\mathbf{Y}|H_1;\underline{\theta}_1)$ denote the probability density functions (pdfs) under both hypotheses, parametrized by the respective parameter vectors $\underline{\theta}_0$ and $\underline{\theta}_1$. In TWRI, the Weibull and Gaussian distributions have been shown in [7] to be accurate models for the pdf under the null and alternative hypothesis, respectively. In this case, $\underline{\theta}_0 = [\lambda, \kappa]^T$ and $\underline{\theta}_1 = [\mu, \sigma]^T$ where λ and κ are the scale and shape parameters of the Weibull pdf, and μ and σ are the mean and standard deviation of the Gaussian pdf.

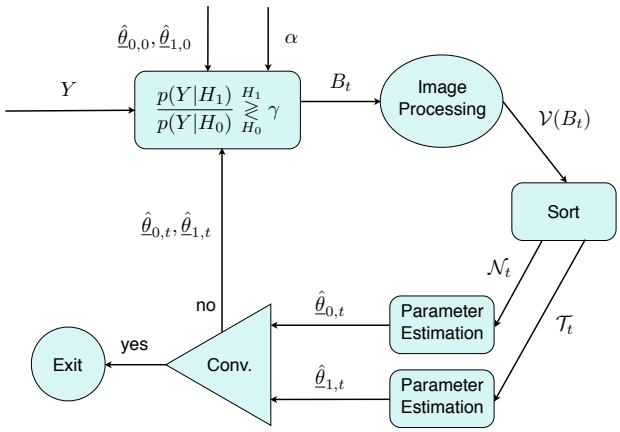

Fig. 1. Iterative detection approach. The aim is to separate the image data into noise and target sets to iteratively improve parameter estimation

In [7], an iterative version of the Neyman-Pearson test (NPT) [9] was proposed as an alternative to classical constant false-alarm rate (CFAR) detection, and will be reviewed in the following. A block diagram is depicted in Figure 1. Given the initial estimates of the parameter vectors $\hat{\underline{\theta}}_{0,0}$ and $\hat{\underline{\theta}}_{1,0}$ (the second index 0 denoting the 0-th, i.e., initial iteration step) as well as a false-alarm rate α to be achieved, the NPT can be performed as,

$$\frac{p(Y|H_1;\hat{\underline{\theta}}_{1,0})}{p(Y)|H_0;\hat{\underline{\theta}}_{0,0})} \underset{H_0}{\overset{H_1}{\gtrless}} \gamma \tag{2}$$

where γ is obtained from α by integrating over the pdf of the likelihood ratio under the null hypothesis [9]. The resulting binary image $\mathbf{B}_0$, which is a first indication of the presence and absence of targets, prone to false alarms and missed detection. An optimal image processing step that aims at removing those false alarms and missed detection in the image domain is followed. The output of the image processing step is a cleaned image $\mathcal{V}(\mathbf{B}_0)$ which now can be used to separate the image data into two disjoint target and noise sets $\mathcal{T}_0$ and $\mathcal{N}_0$. Based on these sets, parameter estimation can be performed to obtain improved parameter estimates $\hat{\underline{\theta}}_{0,1}$ and $\hat{\underline{\theta}}_{1,1}$ which are forwarded to the NPT. The iterative procedure is stopped after a maximum number of iterations or when a vanishing difference in the parameter estimates is achieved.

The image processing step is of high importance in the iterative detection framework. In [10, 8], it was shown that morphological opening and closing operations can successfully separate the image data into noise and target sets.

3. ENHANCED DETECTION OF TARGETS BASED ON OPTIMAL STRUCTURING ELEMENTS

The detector from Section 2 has the advantage that it adapts the parameter vectors to unknown and changing image statistics without making assumptions on the actual type of target. As such it can be seen as a general target detector. In the area of TWRI, one is typically interested in few targets only, e.g., humans and weapons. This means that the vast amount of reflections stemming from the scene hidden behind the wall may not be of interest to the image analyst.

The question thus arises: What if we are interested in a specific class of targets, say humans. How can we extend the approach from Section 2 such that prior knowledge on a specific target can be incorporated? To answer this question, we propose to follow the same iterative detection framework as in [10, 8], but adapt the optimization with respect to the target of interest so as to improve detectability.

Let $\mathbf{Y}^r$, $r = 1, ..., R$ denote a set of R acquired TWRI images of the target of interest which in the following will be denoted as the training set. Based on the target shape in every $\mathbf{Y}^r$, $r = 1, ..., R$ a binary template E_B can be extracted that best represents the target of interest. Note that, as opposed to the optimization scheme from [8, 10], this template is no longer restricted to circular shapes but can take arbitrary shapes. The template E_B then forms the basis of a family of structuring elements $\{E_B^q\}_{q=1}^Q$ by using dilation in both image dimensions. An example of a structuring element with the respective family of elements is depicted in Figure 2.

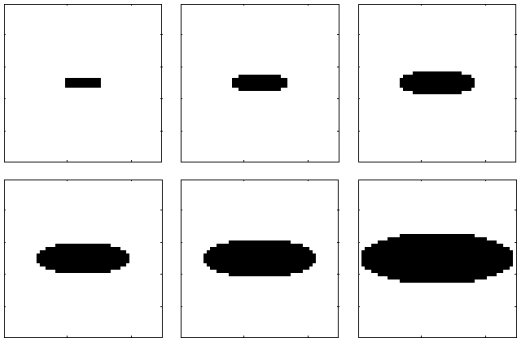

Fig. 2. Exemplary family of structuring elements

Given a family of structuring elements, one can now run the iterative detector from Section 2 with every possible element E_B^q, $q = 1, ..., Q$ and perform optimization similar to

the approach in [8] as,

$$\hat{E} = \arg\min_{E_B^q} \Big(\mathrm{MSE}\left[\tilde{f}_T(y), p(y|H_1;\hat{\underline{\theta}}_1) \mid E_B^q\right] + \mathrm{MSE}\left[\tilde{f}_N(y), p(y|H_0;\hat{\underline{\theta}}_0) \mid E_B^q\right]\Big) \quad (3)$$

where MSE denotes the mean square error and $\tilde{f}_N(y)$ and $\tilde{f}_T(y)$ are nonparametric estimates of the pdfs of the noise and target set, respectively. The pdfs $\tilde{f}_N(y)$ and $\tilde{f}_T(y)$ can be estimated via kernel density estimation as

$$\tilde{f}_N(y) = \frac{1}{hN_0} \sum_{n(u)\in\mathcal{N}} Q\left(\frac{y-n(u)}{h_B}\right) \quad (4)$$

$$\tilde{f}_T(y) = \frac{1}{hT_0} \sum_{t(v)\in\mathcal{T}} Q\left(\frac{y-t(v)}{h_B}\right) \quad (5)$$

where $Q(\cdot)$ and h denote the kernel function and bandwidth, respectively. Further, $n(u)$ and $t(v)$ with $u = 0, ..., N_0 - 1$ and $v = 0, ..., T_0 - 1$ denote the elements of $\mathcal{N}$ and $\mathcal{T}$, respectively, with N_0 and T_0 being the number of elements in each set. Loosely spoken, Equation (3) states that one should choose the structuring element that yields noise and target sets that are (in the mean square sense) in agreement with the postulated pdfs, e.g. the Weibull and Gaussian model for TWRI. There are generally two possibilities of choosing an incorrect structuring element:

- The structuring element is chosen too small. Thus, the nonparametric pdf estimate of the target set $\tilde{f}_T(y)$ will be distorted due to false alarms and as such strongly differs from the parametric pdf estimate $p(y|H_1;\hat{\underline{\theta}}_1)$
- The structuring element is chosen too large. In this case, the nonparametric noise pdf estimate $\tilde{f}_N(y)$ will be distorted due to missed detections and thus strongly differs from the parametric counterpart $p(y|H_0;\hat{\underline{\theta}}_0)$

Both cases yield an increase in the MSE between the nonparametric and parametric pdf estimates. Given the optimal structuring element $\hat{E}$, as per Equation (3), the morphological operations performed in the image processing step (see Figure 1) correspond to opening and dilation, i.e.

$$\mathcal{V}(B_t) = (B_t \circ \hat{E}) \otimes \hat{E} \quad (6)$$

which as proven in [8] separates noise and target sets under mild conditions.

4. EXPERIMENTAL RESULTS

For experimental validation of the proposed detector, we consider the problem of detecting a human behind a wall. The experiment is shown in Figure 3 where a 1.85 meter human (C. Debes) is placed at 2.5 m behind a concrete wall of thickness 0.15 m and dielectric constant 7.66. The back and side walls are covered with absorbers, such that no multipath due to these walls is expected. The floor is not covered with absorbers and will yield a ghost target due to multipath propagation that appears in the resulting image after beamforming.

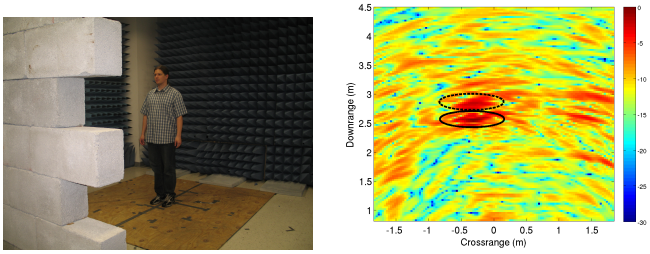

Fig. 3. Experimental setup and resulting B-Scan after wideband sum-and-delay beamforming

The scene is imaged using a 57 element line array at 1.22 m above ground, synthesized using a single antenna element in motion. The interelement spacing is 2.2 cm. A stepped frequency continuous-wave (CW) approach is considered to emulate a wideband pulse. The bandwidth is $0.8 - 3.1$ GHz, achieved by 801 stepped frequencies. Image formation is performed by using the wideband sum-and-delay beamforming approach from [11] which is a nearfield beamformer in the time-domain that compensates for refraction effects which occur by propagation through the wall. As in [11], we considered background subtraction which effectively removes primary wall reflections.

The corresponding B-Scan (twodimensional crossrange vs. range cut at the array height) is depicted on the right hand side of Figure 3. The human target return can be seen at approx. 2.5 m downrange and $0-0.5$ m crossrange (marked by a solid ellipse). The corresponding shadow which appears due to multipath propagation from the floor shows approx. 0.3 m behind the actual target and is marked by a dotted ellipse. It is noted that the appearance of the shadow is not an unwanted effect but can help for target detection. In other words: The appearance of a shadow behind the actual target confirms the target presence.

We now perform target detection as described in Section 2 with a false-alarm rate of 1% using the Weibull and Gaussian pdfs to respectively describe noise and target data. The generalized likelihood ratio test (GLRT) was used to initialize the iterative detector. A circular structuring element with varying diameter as in [8] is chosen to perform the optimization as per Equation (3). The detection result is depicted in Figure 4. The circular structuring element is not optimal for detecting the human. The choice of a suboptimal structuring element yields pixel allocation errors and thus distortions in the estimation of the target and noise pdfs. As a result, the detector tends to converge to a lower threshold, yielding an increase in the false-alarm rate as clearly seen in Figure 4.

When using the enhanced detection approach as detailed

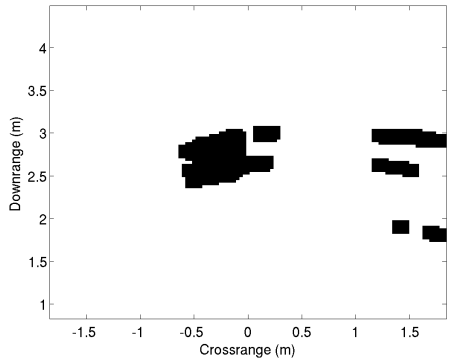

Fig. 4. Detection result, $\alpha = 0.01$. A non-optimal (circular) structuring element is considered.

in Section 3, we are able to optimize the structuring element not to a general target class, but rather to the specific target class of interest, which, in this case, is a human. An elliptic family of structuring elements, similar to Figure 2 is chosen, approximating possible human and shadow returns. The choice of a family of structuring elements rather than a single structuring element, implicitly compensates for resolution effects in the nearfield, considered here. It incorporates the fact that a target standing closer to the wall occupies more pixels than the same target at a longer distance. The detection result can be seen in Figure 5. The target return and shadow are clearly detected, at the same time all false-alarms from Figure 4 are eliminated.

It is noted that the proposed detection scheme can only be used when prior knowledge of the specific target geometry, e.g., by training or electromagnetic simulations, is available. In the case where no such knowledge is available, one should resort to the general target detector [8].

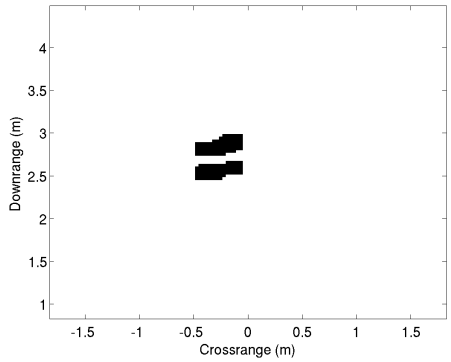

Fig. 5. Detection result, $\alpha = 0.01$. An optimal template-based structuring element is considered.

5. CONCLUSION

A novel image domain-based target detection approach for Through-the-Wall Radar Imaging was proposed. The concept of optimizing morphological structuring elements with respect to a specific target of interest is introduced. We focused on the detection of humans behind walls. The performance of the proposed technique is shown using real data examples. It was demonstrated how the prior knowledge of human target and shadow shapes in the radar image can be used to improve the final detection result.

6. REFERENCES

[1] M. G. Amin, Ed., *Through-the-Wall Radar Imaging*, CRC Press, 2010.

[2] M. Amin and K. Sarabandi (Guest Editors), "Special issue on remote sensing of building interior," *IEEE Transactions on Geoscience and Remote Sensing*, vol. 47, no. 5, 2009.

[3] J. Moulton, S. Kassam, F. Ahmad, M. Amin, and K. Yemelyanov, "Target and change detection in synthetic aperture radar sensing of urban structures," in *Proc. IEEE Radar Conf.*, 2008, pp. 1–6.

[4] A. R. Hunt, "Use of a frequency-hopping radar for imaging and motion detection through walls," *IEEE Trans. on Geoscience and Remote Sensing*, vol. 47, no. 5, pp. 1402–1408, 2009.

[5] F. Soldovieri, R Solimene, and R. Pierri, "A simple strategy to detect changes in through-the-wall imaging," *Progress in Electromagnetics Research M*, vol. 7, pp. 1–13, 2009.

[6] N. Maaref, P. Millot, P. Pichot, and O. Picon, "A study of UWB FM-CW radar for the detection of human beings in motion inside a building," *IEEE Transactions on Geoscience and Remote Sensing*, vol. 47, no. 5, pp. 1297–1300, 2009.

[7] C. Debes, M.G. Amin, and A.M. Zoubir, "Target detection in single- and multiple-view through-the-wall radar imaging," *IEEE Transactions on Geoscience and Remote Sensing*, vol. 47(5), pp. 1349 – 1361, 2009.

[8] C. Debes, J. Riedler, A. M. Zoubir, and M. G. Amin, "Adaptive target detection with application to through-the-wall radar imaging," *IEEE Transactions on Signal Processing*, vol. 58, no. 11, pp. 5572–5583, 2010.

[9] S.M. Kay, *Fundamentals of Statistical Signal Processing, Volume 2: Detection Theory*, Prentice Hall, 1998.

[10] C. Debes, J. Riedler, M.G. Amin, and A.M. Zoubir, "Iterative target detection approach for through-the-wall radar imaging," in *Proc. of the IEEE International Conference on Acoustics, Speech and Signal Processing*, 2009, pp. 3061 – 3064.

[11] F. Ahmad and M.G. Amin, "Multi-location wideband synthetic aperture imaging for urban sensing applications," *Journal of the Franklin Institute*, vol. 345, no. 6, pp. 618–639, 2008.